International Journal for Multiscale Computational Engineering, 2(3)377-400(2004)

Determination of the Material Intrinsic Length Scale of Gradient Plasticity Theory

Rashid K. Abu Al-Rub & George Z. Voyiadjis*

Department of Civil and Environmental Engineering
Louisiana State University Baton Rouge, LA 70803

ABSTRACT

The enhanced gradient plasticity theories formulate a constitutive framework on the continuum level that is used to bridge the gap between the micromechanical plasticity and the classical continuum plasticity. The later cannot predict the size effects since it does not posses an intrinsic length scale. To assess the size effects, it is indispensable to incorporate an intrinsic material length parameter ℓinto the constitutive equations. However, the full utility of gradient-type theories hinges on one's ability to determine the constitutive length-scale parameter ℓ that scales the gradient effects. Thus, the definition and magnitude of the intrinsic length scale are keys to the development of the new theory of plasticity that incorporates size effects. The classical continuum plasticity is also unable to predict properly the evolution of the material flow stress since the local deformation gradients at a given material point are not accounted for. The gradient-based flow stress is commonly assumed to rely on a mixed type of dislocations: those that are initially randomly or statistically distributed, which are referred to as statistically stored dislocations (SSDs), and those formed to account for the additional strengthening mechanism associated with the deformation gradients, which are referred to as geometrically necessary dislocations (GNDs). In this work two micromechanical models to assess the coupling between SSDs and GNDs are discussed. One in which the SSDs and GNDs are simply summed (model-I) and one in which, implicitly, their accompanying strength are added (model-II). These two dislocation interaction models, which are based on Taylor's hardening law, are then used to identify the deformation-gradient-related intrinsic length-scale parameter ℓ in terms of measurable microstructural physical parameters. The paper also presents a method for identifying the material intrinsic length parameter ℓ from micro hardness results obtained by conical or pyramidal indenters.

KEY WORDS

Gradient plasticity; size effects; intrinsic material length scale; statistically stored dislocations; geometrically necessary dislocations; microhardness

*Corresponding author: Voyiadjis@eng.lsu.edu

1. INTRODUCTION

Experimental work on particle-reinforced composites has revealed that a substantial increase in the macroscopic flow stress can be achieved by decreasing the particle size while keeping the volume fraction constant [1–7]. A similar strengthening effect associated with decreasing the diameter of thin wires in microtorsion tests and thickness of thin beams in microbending tests has been reported by Fleck *et al*. [8] and Stolken and Evans [9], respectively. Moreover, micro- and nanoindentation tests have shown that the material hardness increases with decreasing indentation size [10–14]. These experiments have shown an increase in yield strength with decreasing size at the micron and submicron scales. The mechanical properties, such as flow stress or hardness, in metallic materials whether in simple tension, torsion, bending, or indentation testing, are size dependent. The classical continuum plasticity theory [15] cannot predict this size dependency. On the other hand, it is still not possible to perform quantum and atomistic simulations on realistic time and structures. Moreover, the emerging area of nanotechnology exhibits important differences that result from continuous modification of characteristics with changing size. These differences cannot be explained by traditional models and theories. Much is known about the physical properties and behavior of isolated molecules and bulk materials; however, the properties of matter at the nanoscale cannot necessarily be predicted from those observed at larger or smaller scales. However, this problem can be resolved by regularizing or adding an intrinsic material length scale to the continuum. A continuum plasticity theory (but not classical plasticity), therefore, is needed to bridge the gap between the classical continuum plasticity theory and the classical dislocation mechanics.

In the last ten years, a number of authors have physically argued that the size dependence of the material mechanical properties results from an increase in strain gradients inherent in small localized zones, leading to geometrically necessary dislocations that cause additional hardening [8, 10-12, 16]. Material deformation in metals enhances the dislocation formation, motion, and storage. Dislocation storage causes material hardening. The stored dislocations, generated by trapping each other in a random way, are referred to as statistically stored dislocations (SSDs), while the stored dislocations that relieve the plastic deformation incompatibilities within the polycrystal caused by nonuniform dislocation slip are called geometrically necessary dislocations (GNDs); their presence causes additional storage of defects and increases the deformation resistance by acting as obstacles to the SSDs [17]. SSDs are believed to be dependent on the equivalent plastic strain, while the density of GNDs is directly proportional to the gradient of the equivalent plastic strain [16, 18, 19]. During the last decade, the so-called strain gradient plasticity theories have been modified based on the concept of geometrically necessary dislocations in order to characterize the size effects. A length scale enters into the theory, but the discrete dislocation origin is rarely clear and its value is a free parameter.

The enhanced gradient plasticity theories with length scales formulate a constitutive framework on the continuum level that is used to bridge the gap between different physical scale levels while it is still not possible to perform quantum and atomistic simulations on realistic time and structures [20]. This will reduce the computational cost, the prototyping costs, and time to the market. A variety of different gradient-enhanced theories are formulated in a phenomenological manner to address the aforementioned size effects through incorporation of intrinsic length-scale measures in the constitutive equations, mostly based on continuum-mechanics concepts. Moreover, the

gradient theories are nonlocal in the sense that the interstate variable at any location within a solid does not depend only on the state at that location, as in conventional plasticity theory, but also on the state at any other point within the solid. Gradient approaches typically retain terms in the constitutive equations of higher-order gradients with coefficients that represent length-scale measures of the deformation microstructure associated with the nonlocal continuum. Aifantis [21] was one of the first to study the gradient regularization in solid mechanics. The gradient methods suggested by Lasry and Belytschko [22] and Mühlhaus and Aifantis [23] provide an alternative approach to the nonlocal integral equations [24–26]. The gradient terms in several plasticity models are introduced through the yield function [7, 8, 17, 19, 21, 23, 27, 28]. The gradient concept has been extended to the gradient damage theory that has been developed for isotropic damage [29] and for anisotropic damage [30–34]. The gradient plasticity theories have given reasonable agreements with the aforementioned size dependence encountered in composite material experiments [19, 35–39], micro- and nanoindentation experiments [17, 40–45] as well as with the microbend and microtwist experiments [17, 46]. There are also many gradient-enhanced models that were proposed as a localization limiter, i.e., in order to avoid a spurious solution of the localization problems and excessive mesh dependence in conventional plasticity [21–23, 27, 31–34, 47, 48].

Although there has been a tremendous theoretical work to understand the physical role of the gradient theory, this research area is still in a critical state with numerous controversies. Moreover, most of the computational applications of gradient theories focus on the qualitative behavior rather than both the qualitative and quantitative behaviors. This is due, to some extent, to the difficulty in calibration of the different material properties associated with the gradient-dependent models, which is impossible for certain cases, but, more importantly, have been due to the difficulty of carrying out truly definitive experiments on critical aspects of the evolution of the dislocation, crack, and void structure. Furthermore, it is believed that the calibration of the constitutive coefficients of a gradient-dependent model should not only be based on stress-strain behavior obtained from macroscopic mechanical tests, but should also draw information from micromechanical gradient-dominant tests, such as micro- and nanoindentation tests, microbend tests, and/or microtorsion tests, accompained by metallographic studies and stereology-based quantification methods using tomography images. However, indentation experiments are more attractive because they are the most controllable method to examine the plastic behavior of metals under the indenter [49]. From dimensional consideration, in gradient-type plasticity theories, length scales are introduced through the coefficients of spatial gradients of one or more internal variables. Hence the full utility of the gradient-based models in bridging the gap between modeling, simulation, and design of products hinges on one's ability to determine the constitutive length parameter that scales the gradient effects. The work we report here aims at remedying this situation.

Micro- and nanoindentation are widely used experimental methods to probe mechanical properties of materials at micron or submicron scales. As opposed to the nonuniform deformation encountered by indentation tests, the material properties of gradient theories cannot be effectively determined using a typical tension test, where uniform deformation is encountered. The study of Begley and Hutchinson [42] and Shu and Fleck [41] indicated that indentation experiments might be the most effective test for measuring the length-scale parameter ℓ. However, it appears that few re-

searchers have considered the identification of the material intrinsic length-scale ℓ of gradient-enhanced theories from measurements of indentation tests. Nix and Gao [40] estimated the material length-scale parameter ℓ from the microindentation experiments of McElhaney *et al*. [13] to be $\ell = 12\ \mu m$ for annealed single crystal copper and $\ell = 5.84\ \mu m$ for cold-worked polycrystalline copper. Yuan and Chen [44] proposed that the unique intrinsic material length parameter ℓ can be computationally determined by fitting the Nix and Gao [40] model from microindentation experiments and they have identified ℓ to be $\ell = 6\ \mu m$ for polycrystal copper and $\ell = 20\ \mu m$ for single crystal copper. By fitting microindentation hardness data, Begley and Hutchinson [42] have estimated that the material length scale associated with the stretch gradients ranges from 0.25 to $0.5\ \mu m$, while the material lengths associated with rotation gradients are on the order of $4.0\ \mu m$. Other tests also have been used to determine ℓ. Based on Fleck *et al*. [8] microtorsion test of thin copper wires and Stolken and Evans [9] microbend test of thin nickel beams, the material length parameter is estimated to be $\ell = 4\ \mu m$ for copper and $\ell = 5\ \mu m$ for nickel. When considering the microstructure with localization zones, gradient-dependent behavior is expected to play an important role once the length scale associated with the local deformation gradients become sufficiently large when compared with the controlling microstructural feature (e.g., mean spacing between inclusions relative to the inclusion size when considering a microstructure with dispersed inclusions, size of the plastic process zone at the front of the crack tip, the mean spacing between dislocations, the grain size, etc.). All the aforementioned gradient plasticity theories degenerate to classical plasticity when the controlling microstructural feature becomes much larger than the intrinsic material length scale ℓ. Therefore, the transition from the discrete dislocation structure to a continuum description is possible when the length scale is sufficiently large compared to the characteristic length of the dislocation distribution. However, there is still a fundamental issue that needs to be resolved first: how to retain the length scale from the characteristic discrete dislocation scale in the continuum description? In spite of the fact of the crucial importance of the length-scale parameter in gradient theory of plasticity, very limited work focused on the physical origin of this length scale. In this work we are aiming at remedying this situation by finding this parameter from a set of dislocation mechanics-based considerations. The definition and magnitude of the length scale are thus keys to the modeling, simulation, and design of emerging micro- and nanosystems [20].

Recently, Voyiadjis *et al*. [34] developed a general thermodynamic framework for the analysis of heterogeneous media that assesses a strong coupling between rate-dependent plasticity and anisotropic rate-dependent damage. They showed that the variety of plasticity and damage phenomena at small-scale level dictate the necessity of more than one length parameter in the gradient description. They expressed these material length-scale parameters in terms of macroscopic measurable material properties. However, this work concerns with the identification of the material intrinsic length-scale parameter ℓ for gradient isotropic hardening plasticity. This can be effectively done through establishing a bridge between the plasticity at the micromechanical scale and with the plasticity at the macromechanical scale [50]. This bridge is characterized by the gradient theory of plasticity. A constitutive framework is formulated using two micromechanical models that assess, in a different manner, the coupling between statistically stored dislocations (SSDs) and geometrically necessary dislocations (GNDs). One in which the SSDs and GNDs are simply summed (model-I) and one in which, implicitly, their

accompanying strength are added (model-II). These two micromechanical models, which are based on Taylor's hardening law, are used to link the strain-gradient effect at the microscopic scale with the stress-strain behavior of an equivalent continuum with homogenized plastic deformation at the macroscopic level. This constitutive framework yields expressions for the deformation-gradient-related intrinsic length-scale parameter ℓ in terms of measurable microstructural physical parameters. Moreover, we present a method for identifying the material intrinsic length parameter from micro- and nanoindentation tests using conical or pyramidal (e.g., Berkovich and Vickers) indenters. In addition, there are indications that a constant value of the material length scale is not always realistic and that different problems could require different values [46]. The change in length-scale magnitude is physically sound since the continuous modification of material characteristics with time. Some authors argued the necessity of a length-scale parameter in the gradient theories that change with time in order to achieve an efficient computational convergence while conducting multiscale simulations [51]. An evolution equation has been derived for the length-scale parameter that shows that the characteristic material length scale decreases with increasing strain rates, but it increases with temperature decrease.

The overall objective of this paper is to help understand what the basic structure of gradient plasticity theories should be.

2. ISOTROPIC HARDENING

Many researchers tend to write the nonlocal weak form of the conventional effective plastic strain $\widehat{p}$ in terms of its local counterpart p and high-order gradient terms. The following modular generalization of $\widehat{p}$ can then be defined through the modification of that proposed by Fleck and Hutchinson [19],

$$\widehat{p} = [p^{\gamma} + (\ell\eta)^{\gamma}]^{1/\gamma}, \tag{1}$$

where ℓ is a length parameter that is required for dimensional consistency and whose physical interpretation will be discussed in detail later in this paper. η is the measure of the effective plastic strain gradient of any order. The superimposed hat denotes the spatial nonlocal operator. γ is a constant, which can be interpreted as a material parameter. Equation (1) ensures that $\widehat{p} \rightarrow p$ whenever $p >> \ell\eta$ and that $\widehat{p} \rightarrow \ell\eta$ whenever $p << \ell\eta$. Two values of γ are generally investigated in the literature: (a) $\gamma = 1$ which corresponds to a superposition of the contributions of the local plastic strain and the higher-order gradients of the plastic strain to the flow stress; and (2) $\gamma = 2$, which since the effective plastic strain scales with the norm of the plastic strain tensor, corresponds to a superposition of the effective plastic strain of the two types of local and nonlocal parts.

Aifantis [21, 52] used the magnitude of the gradient of the conventional effective plastic strain $p = \sqrt{2\varepsilon^p_{ij}\varepsilon^p_{ij}}\Big/3$ as a measure of the strain gradient, with η expressed as follows:

$$\eta = \|\nabla_i p\| = \sqrt{\nabla_k p\, \nabla_k p}, \tag{2}$$

where ∇_k designates the gradient operator, and $\gamma = 1$ in this case.

In the work of de Borst and his coworkers [27, 47] the gradient-dependent plasticity model expresses the flow stress in terms of the second-order gradient of the effective plastic strain such that η is expressed as follows:

$$\ell\eta = \sqrt{\ell^*\, \nabla^2 p}, \tag{3}$$

where ℓ^* is the square of a length parameter associated with second-order gradient and ∇^2 is the Laplacian operator, and $\gamma = 2$ in this case.

In the mechanism-based strain gradient (MSG) plasticity theory [19, 28, 53], the effective strain-gradient is defined in terms of the gradient of the plastic strain tensor ε^p_{ij} as follows:

$$\ell\eta = \sqrt{c_1\eta_{iik}\eta_{jjk} + c_2\eta_{ijk}\eta_{ijk} + c_3\eta_{ijk}\eta_{kji}} \quad (4)$$

so that $\gamma = 1$ and $\eta_{ijk} = \eta_{jik}$ is given as

$$\eta_{ijk} = \varepsilon^p_{ki,j} + \varepsilon^p_{kj,i} - \varepsilon^p_{ij,k} \quad (5)$$

c_1 , c_2 and c_3 scale the three quadratic invariants for the incompressible third-order tensor η_{ijk}, which are determined by matching a series of distinct dislocation models consisting of plane strain bending, pure torsion, and two-dimensional axisymmetric void growth [17, 54], which respectively results in $c_1 = 0$, $c_2 = 1/4$, and $c_3 = 0$, such that Eq. (4) can be written as

$$\eta = \sqrt{\tfrac{1}{4}\eta_{ijk}\eta_{ijk}}\,. \quad (6)$$

Smyshlyaev and Fleck [55] and Fleck and Hutchinson [19, 28] have shown that the incompressible strain-gradient tensor η_{ijk} can be decomposed as

$$\eta_{ijk} = \sum_{m=1}^{3} \eta^{(m)}_{ijk} \quad (7)$$

with

$$\eta^{(1)}_{ijk} = \eta^S_{ijk} - \tfrac{1}{5}(\delta_{ij}\eta^S_{kpp} + \delta_{ik}\eta^S_{jpp} + \delta_{jk}\eta^S_{ipp}) \quad (8)$$

$$\eta^{(2)}_{ijk} = \tfrac{1}{6}\times (e_{ikp}e_{jlm}\eta_{lpm} + e_{jkp}e_{ilm}\eta_{lpm} + 2\eta_{ijk} - \eta_{jki} - \eta_{kij}) \quad (9)$$

$$\eta^{(3)}_{ijk} = \tfrac{1}{6}\times (-e_{ikp}e_{jlm}\eta_{lpm} - e_{jkp}e_{ilm}\eta_{lpm} + 2\eta_{ijk} - \eta_{jki} - \eta_{kij}) + \tfrac{1}{5}(\delta_{ij}\eta^S_{kpp} + \delta_{ik}\eta^S_{jpp} + \delta_{jk}\eta^S_{ipp}) \quad (10)$$

In the above equations, δ_{ij} is the Kronecker delta, e_{ijk} is the permutation tensor, and η^S_{ijk} is the fully symmetric part of η_{ijk},

$$\eta^S_{ijk} = \tfrac{1}{3}\left(\eta_{ijk} + \eta_{jki} + \eta_{kij}\right). \quad (11)$$

Fleck and Hutchinson [19, 28] showed that the effective strain gradient defined in Eq. (4) can be rewritten by substituting Eqs. (7)–(11) as follows:

$$\eta = \sqrt{\frac{1}{\ell^2}\sum_{m=1}^{3} \ell^2_m \eta^{(m)}_{ijk}\eta^{(m)}_{ijk}}, \quad (12)$$

where $\ell^2_1/\ell^2 = c_2 + c_3$, $\ell^2_2/\ell^2 = c_2 - \frac{1}{2}c_3$ and

$$\ell^2_3/\ell^2 = \tfrac{5}{2}c_1 + c_2 - \tfrac{1}{4}c_3. \quad (13)$$

Substituting $c_1 = 0$, $c_2 = 1/4$, and $c_3 = 0$, as reported by Gao *et al*. [17, 54], gives

$$\ell_1 = \ell_2 = \ell_3 = \tfrac{1}{2}\ell \quad (14)$$

Fleck and Hutchinson [19] proposed also to determine these three length parameters from microexperiments. Begley and Hutchinson [42] obtained from fitting their model with the experimental data of bending of ultrathin beams, torsion of thin wires, and microindentation, the following values of the length parameters such that,

$$\ell_1 = \tfrac{1}{8}\ell,\ \ \ell_2 = \tfrac{1}{2}\ell,\ \text{ and }\ \ell_3 = \sqrt{\tfrac{5}{24}}\ell. \quad (15)$$

Two models are proposed in the subsequent sections used to link the strain-gradient effects at the microscopic scale with the stress-strain behavior of an equivalent continuum with homogenized plastic deformation at the macroscopic level. This link is described by the aforementioned gradient theory of plasticity, which is characterized by the general expression defined by Eq. (1).

2.1 Model-I

Taylor's hardening law, which that relates the shear strength to the dislocation density, has been the basis of the mechanism-based strain-gradient (MSG) plasticity theory [17, 40, 43, 54]. It gives a simple description of the dislocation interaction processes at the microscale (i.e., over a scale that extends from about a fraction of a micron to tens of microns). The critical shear stress that is required to untangle the interactive dislocations and to induce a significant plastic deformation is defined as the Taylor flow stress (e.g., [12, 17, 49]):

$$\tau = \alpha G b \sqrt{\rho_T}, \tag{16}$$

where α is an empirical constant usually ranging from 0.1 to 0.5 [18], G is the shear modulus, b is the magnitude of the Burgers vector, and ρ_T is the total dislocation density due to different types of dislocations that cause material hardening. If the von Mises flow rule is assumed, the normal flow stress can then be written as follows:

$$\sigma = \sqrt{3}\,\alpha G b \sqrt{\rho_T}, \tag{17}$$

where σ is the normal flow stress, which is equivalent to the effective stress. For crystalline materials (e.g., face-centered-cubic solids), a more accurate relationship accounting for the so-called Taylor factor [56] between the tensile flow stress and critical resolved shear stress in slip systems is given by $\sigma = 3\,\tau$. The Taylor factor acts as an isotropic interpretation of the crystalline anisotropy at the continuum level. The use of the assumption of isotropy of solids is imperative since we are seeking a continuum description of the discrete dislocations scale. The isotropic hardening law in Eq. (17) is a continuum property, such as the forest hardening that is inherited from a discrete dislocation scale.

Generally, it is assumed that the total dislocation density ρ_T represents the total coupling between two types of dislocations, which play a significant role in the hardening mechanism. Material deformation enhances dislocation formation, motion, and storage. As mentioned dislocation storage causes material hardening. Stored dislocations generated by trapping each other in a random way are referred to as statistically-stored dislocations (SSDs), while stored dislocations required for compatible deformation within the polycrystal are called geometrically-necessary dislocations (GNDs). Their presence causes additional storage of defects and increases the deformation resistance by acting as obstacles to the SSDs [54]. The SSDs are created by homogenous strain and are related to the plastic strain, while the GNDs are related to the curvature of the crystal lattice or to the strain gradients [18, 57]. Plastic strain gradients appear either because of geometry, loading, and/or because of inhomogeneous deformation in the material. Hence, GNDs are required to account for the permanent shape change. The nonlocal effective plastic strain in Eq. (1) is intended to measure the total dislocation density that accounts for both: dislocations that are statistically stored and geometrically necessary dislocations induced by the strain gradients [17, 28].

Gao *et al*. [17, 54] and Fleck and Hutchinson [19] expressed the total dislocation density ρ_T as the sum of the SSD density ρ_S, and GND density ρ_G such that,

$$\rho_T = \rho_S + \rho_G. \tag{18}$$

Other couplings between ρ_S and ρ_G are possible. Fleck and Hutchinson [19] proposed that ρ_T can be expressed as the harmonic sum of ρ_S and ρ_G such that,

$$\rho_T = \sqrt{\rho_S^2 + \rho_G^2}. \tag{19}$$

However, a more general coupling of ρ_S and ρ_G can be proposed in the spirit of Eq. (1) as follows [56]:

$$\rho_T = \left[\rho_S^{\mu} + \rho_G^{\mu}\right]^{1/\mu}, \tag{20}$$

where μ is a constant that can be interpreted as a material parameter similar to the γ constant in Eq. (1). It is obvious from Eqs. (1) and (20) that μ and γ are related to each other. Furthermore, the above expression ensures that $\rho_T \to \rho_S$ whenever $\rho_G << \rho_S$ and that $\rho_T \to \rho_G$ whenever $\rho_S << \rho_G$. Thus, Taylor's hardening law given by Eq. (17) can be rewritten as

$$\sigma = \sqrt{3}\,\alpha G b \left[\rho_S^{\mu} + \rho_G^{\mu}\right]^{1/2\mu}. \tag{21}$$

It is imperative to note that the nonlocal effects associated with the presence of local deformation gradients at a given material point are incorporated into Eq. (21) through GND density [37]. Thus, Eq. (21) constitutes the nonlocal micromechanical plasticity constitutive model similar to the nonlocal macromechanical plasticity expression in Eq. (1). Moreover, at the microscale, where dislocation densities are used as the appropriate variables to describe plastic flow, the introduction of high-order gradient terms in the conventional continuum mechanics has led to bridge the gap between the conventional continuum and the micromechanical plasticity theories. Nix and Gao [40], Gao *et al*. [17, 54], Arsenlis and Parks [16], and Huang *et al*. [53] showed that the gradient in the plastic strain field is accommodated by the geometrically necessary dislocations ρ_G so that the effective strain gradient η, which appears in Eq. (1), can be defined as follows:

$$\eta = \frac{\rho_G\, b}{\bar{r}}. \tag{22}$$

They showed that this expression allows η to be interpreted as the curvature of deformation in bending and twist per unit length in torsion [53]. Whereas, the statistically stored dislocations ρ_S are dependent on the effective plastic strain p. $\bar{r}$ is the Nye factor introduced by Arsenlis and Parks [16] to reflect the scalar measure of GND density resultant from macroscopic plastic strain gradients. For FCC polycrystals, Arsenlis and Parks [16] have reported that the Nye factor has a value of $\bar{r}$ = 1.85 in bending and a value of $\bar{r}$ = 1.93 in torsion. The Nye factor emphasizes the increased concentration of GNDs by affirming that the dislocation density accumulated in a grain at a certain strain is higher once the grain size decreases, which is inherent to the increased inhomogeneous deformation (i.e., strain gradients) within the grain and the accompanying decreasing mean-free path of the dislocations [16]. The Nye factor, therefore, is an important parameter in the predictions of the gradient plasticity theories as compared to the experimental results [17].

The uniaxial flow stress-plastic strain hardening relation without the effects of strain gradients can be identified, in general, as follows (e.g., [40, 44, 54]):

$$\sigma = k\, f\,(p)\,, \tag{23}$$

where k is a measure of the yield stress in uniaxial tension and f is a function of the effective plastic strain p. For the majority of the ductile materials, the function f can be written as a power-law relation (e.g., [58]), such that

$$f\,(p) = p^{1/m}, \tag{24}$$

where $m \geq 1$ is a material parameter that can be determined from a simple uniaxial tension test.

However, since uniaxial tension tests exhibit homogenous deformation, Eq. (23) cannot be used to describe applications where the nonuniform plastic deformation plays an important role (e.g. twisting, bending, deformation of composites, micro- or nanoindentation, etc.). Equation (23) cannot then predict the size dependence of material behavior after normalization, which involves no internal material length scale. Therefore, Eq. (23) should be modified to be able to incorporate the size effects. This can be effectively done by replacing the conventional effective plastic strain measure p by its corresponding nonlocal measure $\widehat{p}$ defined by Eq. (1), such that Eqs. (23) and (24)

can be rewritten as

$$\sigma = k\left[p^{\gamma} + l^{\gamma}\eta^{\gamma}\right]^{1/m\gamma}. \tag{25}$$

This gradient law exactly matches the Fleck-Hutchinson [19] phenomenological law in the case of a single-material length scale, where γ is taken to be 2, but can be generalized to any arbitrary number larger than 1 without destroying the basic theoretical framework. However, in their work η is expressed as an effective strain gradient given by

$$\eta = \sqrt{\tfrac{2}{3}\chi_{ij}\chi_{ij}}, \tag{26}$$

where χ_{ij} is the so-called curvature tensor [19], which is related to the incompressible third-order tensor η_{ijk} [Eq. (5)] by

$$\chi_{ij} = \tfrac{1}{2}e_{iqr}\eta_{jqr}. \tag{27}$$

Moreover, the Fleck and Hutchinson theory [19, 28] considers the strain gradients as internal degrees of freedom and requires thermodynamic work conjugate higher-order stresses, which need additional boundary conditions to be imposed. However, the proposed model in Eq. (25) gives an alternative framework that could model size-dependent plasticity without higher-order stresses or additional boundary conditions, so as to preserve the essential structure of classical plasticity. This approach has the advantages that it is simpler overall and can be easily implemented into existing finite element codes.

It is worth mentioning that Eqs. (21) and (25) imply that plasticity is the macroscopic outcome from the combination of many dislocation elementary properties at the micro- and mesoscopic scale. These two equations, therefore, represent the link of microscale plasticity to the microscopic plasticity. The effective use of this link will be demonstrated in what follows.

Next we use Eq. (25), which expresses the flow stress in the macroscale, along with Taylor's hardening law [Eq. (21)], in the microscale to derive the material-intrinsic length scale for isotropic hardening gradient plasticity in terms of physical microstructural parameters. Bammann and Aifantis [59] defined the plastic shear strain γ^p as a function of the SSD density ρ_S as follows:

$$\gamma^p = bL_S\rho_S, \tag{28}$$

where L_S is the mean spacing between SSDs, which is usually in the order of submicron. Furthermore, Bammann and Aifantis [59] generalized the Orowan's equation (with an orientation factor) of the plastic strain in the macroscopic plasticity theory in terms of the plastic shear strain and an orientation tensor as follows:

$$\varepsilon^p_{ij} = \gamma^p M_{ij}, \tag{29}$$

where M_{ij} is the symmetric Schmidt's orientation tensor. In expressing the plastic strain tensor at the macrolevel to the plastic shear strain at the microlevel, an average form of the Schmidt's tensor is assumed since plasticity at the macroscale incorporates a number of differently oriented grains into each continuum point [52, 60]. Moreover, average values are used for the magnitude of the Burgers vector b and the mean spacing between SSDs L_S .

The flow stress σ is the conjugate of the effective plastic strain variable p in macroplasticity. For proportional, monotonically increasing plasticity, p is defined as

$$p = \sqrt{\tfrac{2}{3}\varepsilon^p_{ij}\varepsilon^p_{ij}}. \tag{30}$$

Hence, utilizing Eqs. (28) and (29) in Eq. (30) one can write p as a function of SSDs as follows:

$$p = bL_S\rho_S\bar{M}, \tag{31}$$

which is referred to as Orowan's equation, where $\bar{M} = \sqrt{2M_{ij}M_{ij}/3}$ can be interpreted as Schmidt's orientation factor, usually taken equal to $1/2$. It is clear from Eq. (31) that the Burgers vector and the dislocation spacing are

two physical length scales that control plastic deformation.

Substituting ρ_G and ρ_S from Eqs. (22) and (31), respectively, into Eq. (21) yields the following expression for the flow stress:

$$\sigma = \alpha G \sqrt{\frac{3b}{L_S \bar{M}}} \left[p^{\mu} + L_s \bar{M}\, \bar{r} \eta^{\mu} \right]^{1/2\mu}. \quad (32)$$

Comparing Eq. (32) with Eq. (25) yields the following relations:

$$\gamma = \mu \ , m = 2, \ \ k = \alpha G \sqrt{\frac{3b}{L_S \bar{M}}},$$
$$\ell = L_S\, \bar{M}\, \bar{r}. \quad (33)$$

The rational for obtaining $\gamma = \mu$ is based on the following argument. The flow strength depends on the total dislocation density ρ_T, as assumed by Eq. (17). One coupling form between ρ_S and ρ_G is presented by Eq. (18) as $\rho_T = \rho_S + \rho_G$ with $\mu = 1$ [17, 19, 54], and that ρ_G and ρ_S are linear in the strain gradient [Eq. (22)] and the effective plastic strain [Eq. (31)], respectively. One concludes then that an appropriate scalar measure of hardening is given by Eq. (25) with $\gamma = \mu = 1$. Moreover, another coupling between ρ_S and ρ_G is presented by Eq. (19) as $\rho_T^2 = \rho_S^2 + \rho_G^2$ with $\mu = 2$ [19], where ρ_S and ρ_G are obtained from Eqs. (31) and (22), respectively. Hence one concludes that the hardening law [Eq. (25)] is appropriately expressed with $\gamma = \mu = 2$. Thus, in general, an appropriate scalar measure of hardening is given by Eq. (25) with $\gamma = \mu$. Furthermore, the condition $m = 2$ is not unreasonable for some materials [40], particularly for some annealed crystalline solids. The phenomenological measure of the yield stress in uniaxial tension k and the microstructure length-scale parameter ℓ are now related to measurable physical parameters L_S, b, $\bar{r}$, $\bar{M}$, α, and G. Moreover, by substituting $L_S\, \bar{M}$ from Eq. $(33)_3$ into Eq. $(33)_4$ one can obtain a similar relation for ℓ as proposed by Gao *et al*. [17] such that:

$$\ell = 3\alpha^2 b \bar{r} \left(\frac{G}{k} \right)^2. \quad (34)$$

We note that the above equation implies that the length-scale parameter may vary with the strain-rate and temperature for a given material for the case $k = \widehat{k}(\dot{p}, T)$, where $\dot{p} = \sqrt{2\dot{\varepsilon}_{ij}^p \dot{\varepsilon}_{ij}^p \big/ 3}$. However, for most metals, the flow stress increases with the strain rate and decreases with temperature increase. Thus causing the intrinsic material length scale to decrease with increasing strain rates and to increase with temperature decrease. However, opposite behavior is concluded for the gradient term η.

2.2 Model-II

Another approach to form the coupling between SSDs and GNDs is to assume that the overall flow stress τ has two components; one arising from SSDs τ_S and a component due to GNDs τ_G [61]. The following general function for τ is then chosen as follows:

$$\tau = \left[\tau_S^{\beta} + \tau_G^{\beta} \right]^{1/\beta} \quad (35)$$

with τ_S and τ_G are given by Taylor's hardening law as follows:

$$\tau_S = \alpha_S G b_S \sqrt{\rho_S}, \quad (36)$$

$$\tau_G = \alpha_G G b_G \sqrt{\rho_G}, \quad (37)$$

where b_S and b_G are the magnitudes of the Burgers vectors associated with SSDs and GNDs, respectively, and α_S and α_G are statistical coefficients, which account for the deviation from regular spatial arrangements of the SSD and GND populations, respectively. For an impenetrable forest, it is reported that $\alpha_S \approx 0.85$ [66] and $\alpha_G \approx 2.15$ [37].

This general form ensures that $\tau \to \tau_S$ whenever $\tau_S >> \tau_G$ and that $\tau \to \tau_G$whenever $\tau_S <<$

τ_G . Two values of β are generally investigated in the literature: (a) $\beta = 1$, which corresponds to a superposition of the contributions of SSDs and GNDs to the flow stress (e.g., [61]); and (2) $\beta = 2$, which, since the flow stress scales with the square root of dislocation density, corresponds to the superposition of the SSD and GND densities (e.g., [37]). Moreover, Eq. (35) constitutes the nonlocal micromechanical plasticity constitutive model due to the presence of GNDs similar to the nonlocal macromechanical plasticity constitutive model defined by Eq. (25) due to the presence of strain gradients η.

Expressing Eq. (35) in terms of Eqs. (36) and (37) yields a general expression for the overall flow stress in terms of SSD and GND densities, such that

$$\tau = \alpha_S G b_S \left[\rho_S^{\beta/2} + \left(\frac{\alpha_G b_G}{\alpha_S b_S} \right)^{\beta} \rho_G^{\beta/2} \right]^{1/\beta}. \quad (38)$$

Alternatively, Eq. (38) can be redefined in terms of an equivalent total dislocation density ρ_T as follows:

$$\rho_T = \left[\rho_S^{\beta/2} + \left(\frac{\alpha_G^2 b_G^2}{\alpha_S^2 b_S^2} \rho_G \right)^{\beta/2} \right]^{2/\beta} \quad (39)$$

so that

$$\tau = \alpha_S G b_S \sqrt{\rho_T}. \quad (40)$$

It is important to emphasize once again that the nonlocal effects associated with the presence of local deformation gradients at a given material point are incorporated into Eq. (40) through the GNDs density.

Substituting ρ_G and ρ_S from Eqs. (22) and (31), respectively, into $\sigma = \sqrt{3}\tau$, where τ is given by Eq. (40), yields the following expression for the flow stress:

$$\sigma = \alpha_S G \sqrt{\frac{3 b_S}{L_S \bar{M}}} \times \left[p^{\beta/2} + \left(\frac{\alpha_G^2 b_G L_s \bar{M}\, \bar{r}}{\alpha_S^2 b_S} \eta \right)^{\beta/2} \right]^{1/\beta}. \quad (41)$$

Note that we set $b = b_G$ in Eq. (22) and $b = b_S$ in Eq. (31) since the plastic strain gradient and the plastic strain are related to the SSDs and GNDs, respectively. Comparing Eq. (41) with Eq. (25) yields the following relations:

$$\gamma = \beta/2, m = 2, k = \alpha_S G \sqrt{\frac{3 b_S}{L_S \bar{M}}},$$
$$\ell = (\alpha_G/\alpha_S)^2 (b_G/b_S) L_S \bar{M}\, \bar{r}. \quad (42)$$

Moreover, by substituting $L_S \bar{M}$ from Eq. $(42)_3$ into Eq. $(42)_4$ one can obtain a relation for ℓ as function of the shear modulus G and the thermal stress k, such that

$$\ell = 3\alpha_G^2 b_G \bar{r} \left(\frac{G}{k} \right)^2. \quad (43)$$

It is noteworthy to mention that by comparing the results retained from model-I and model-II, Eqs. (42) and (44) with Eqs. (33) and (34), one can notice that model-II gives qualitatively more general and rational expressions for k and ℓ. k is essentially controlled by SSDs and ℓhas a more general form as obtained from model-II, Eq. $(42)_4$, as compared to ℓ obtained from model-I, Eq. $(33)_4$. Moreover, Eq. (44) shows that the material length scale is directly related to the storage of geometrically necessary dislocations. However, both models are identical when $\alpha_S = \alpha_G = \alpha$, $b_S = b_G = b$, and $\beta = 2\mu$. Moreover, the condition $m = 2$ is not unreasonable for some materials as we mentioned earlier. However, the authors believe that the origin of this condition, as it is concluded from the mathematical setup of model-I and model-II, comes out from the assumption that Taylor's flow stress is directly proportional to the square root of the dislocation density (i.e., $\tau \infty \sqrt{b^2 \rho_T}$, which can be rewritten as $\rho_T^{1/m}$ with $m = 2$. For more generality, we can assume that $\tau \propto (b^2 \rho_T)^{1/m}$ with $m \geq 1$. This is not the subject of this work, but further study needs to be carried out to show the importance of this found.

3. IDENTIFICATION FROM MICRO-HARDNESS EXPERIMENTS

The conventional hardness test is one of the oldest and simplest methods of material quality evaluation. Tabor [67] and Atkins and Tabor [68] showed in their experiments that the elasto-plastic material response in tensile testing could be correlated to the response in conical/pyramidal (e.g., Berkovich and Vickers) or spherical (or Brinell) indentation. The fundamental parameters for indentation tests by conical/pyramidal indenter are: the force applied to the indenter P, the residual contact radius of indentation a, the contact pressure (hardness) $H = P/\pi a^2$, the permanent penetration depth h, the total penetration depth h_t, and the indenter geometry (i.e., the angle between the surface of the conical indenter and the plane of the surface θ). The unloading process in the indentation experiment is the most important for a proper specification of these geometric parameters. Thus, the residual penetration depth h and contact radius a should be used as measurable data in the hardness H calculation.

It is well known by now that indentation tests at scales on the order of one micron have shown that measured hardness increases significantly with decreasing indent size. This has been attributed to the evolution of geometrically necessary dislocations associated with gradients. Next we present a simple procedure to identify the intrinsic material-length parameter that scales the effect of GNDs using conical or pyramidal indenter.

Consider the indentation by a rigid cone, as shown schematically in Fig. 1. First, in this analysis we assume that the density of geometrically necessary dislocations is integrated by the geometry of the indenter and the indentation is accommodated by circular loops of GNDs with Burgers' vectors normal to the plane of the surface. Since model-II gives more general expressions than model-I, we assume, in what follows, that the densities of statistically stored dislocations and geometrically necessary dislocations are coupled as proposed in model-II [Eq. (35)]. Based on the simple model of GNDs developed first by Stelmashenko et al. [10] and DeGuzman *et al*. [11] and recently recalled by Nix and Gao [40], an analytical expression for the density of GNDs (ρ_G) under the conical indenter can be obtained in terms of the material properties and the conical indenter geometry. The development of ρ_G is presented in detail here for the convenience of the reader. Following Begley and Hutchinson [42], the indentation profile in the unloaded configuration can be described by

$$w(r) = r(\tan\theta) - h \quad for \quad 0 \le r \le a \qquad (44)$$

where h is the indentation depth and θ is the angle between the surface of the conical indenter and the plane of the surface. This angle is related to the indentation depth h and the radius of the contact area of the indentation a by $\tan\theta = h/a$ (see Fig. 1). Both h and a are measured in the unloaded configuration and characterized as the residual values after unloading. If we assume that the individual dislocation loops of GNDs as being spaced equally along the surface of the indentation, then it is easy to show that

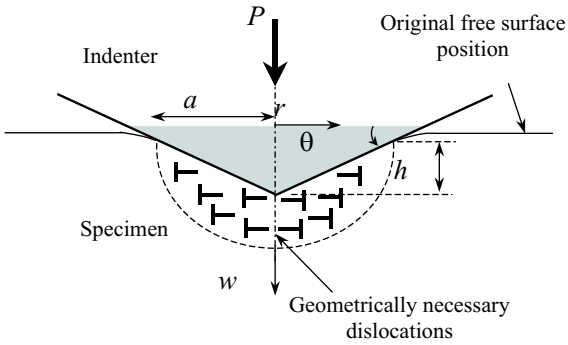

FIGURE 1. Axisymmetric rigid conical indenter. Geometrically necessary dislocations created during the indentation process

$$\left|\frac{dw}{dr}\right| = \frac{b_G}{s} = \tan\theta = \frac{h}{a}, \quad s = \frac{b_G a}{h}, \tag{45}$$

where s is the mean spacing between individual slip steps on the indentation surface. If L is the total length of the injected loops, then between r and $r + dr$ we have

$$dL = 2\pi r \frac{dr}{s} = 2\pi r \frac{h}{b_G a} dr. \tag{46}$$

Integrating from 0 to a gives the total length of dislocation loops as

$$L = \int_o^a 2\pi r \frac{h}{b_G a} dr = \frac{\pi a h}{b_G}. \tag{47}$$

Moreover, it is assumed that the dislocation evolution during indentation is primarily governed by a large hemispherical volume V that scales with the contact radius a around the indentation profile. One can then assume that all the injected loops remain within the hemispherical volume V such that:

$$V = \frac{2}{3}\pi a^3. \tag{48}$$

Therefore, the density of geometrically necessary dislocations becomes

$$\rho_G = \frac{L}{V} = \frac{3}{2 b_G h} \tan^2\theta. \tag{49}$$

In the early hardness experiments, it was concluded that the relation between the hardness H and the permanent penetration depth h follows a power law. Making use of this observation, Tabor [67] specified the mapping from the hardness-indentation depth curve ($H-h$ curve) to the tensile stress-plastic strain curve ($\sigma - p$), such that one can assume the following:

$$H = \kappa\sigma, \tag{50}$$

where κ is the Tabor's factor of $\kappa = 2.8$ and c is a material constant with a value of $c = 0.4$ [67]; while corresponding numerical result from Biwa and Storakers [69] is $\kappa = 3.07$. This relation has been extensively verified and used by many authors (e.g., [40, 49, 58, 69–75]).

Moreover, Based on the assumption of a self-similar deformation field [69, 76], it was shown by using the conical/pyramidal indenter that the displacement is proportional to the indentation depth h. Based on this observation, Xue *et al*. [77] showed from numerical experiments that the strain field should depend only on the normalized indentation depth, h/a, and the normalized position (x/a, y/a, z/a, where x, y, and z are the Cartesian coordinates such that one can assume that the effective plastic strain p is defined by

$$p = c\left(\frac{h}{a}\right) = c\tan\theta \tag{51}$$

where c is a material constant on the order of 1.0 [77].

Considering the results derived from model-II, the substitution of Eq. (38) into Eq. (50) with $\sigma = \sqrt{3}\tau$ and Eqs. (51) and $(42)_4$ into Eq. (31), yield the following expressions for hardness H and statistically stored dislocations (ρ_S), respectively, as follows:

$$H = \sqrt{3}\,\kappa\alpha_S G b_S \left[\rho_S^{\beta/2} + \left(\frac{\alpha_G b_G}{\alpha_S b_S}\right)^{\beta} \rho_G^{\beta/2}\right]^{1/\beta}, \tag{52}$$

$$\rho_S = \frac{c\bar{r}\alpha_G^2 b_G \tan\theta}{\ell b_S^2 \alpha_S^2}. \tag{53}$$

Note that we set $b = b_S$ in Eq. (31) since the plastic strain is related to the SSDs. Moreover, we can define the macrohardness H_o as the hardness that would arise from SSDs alone in the absence of strain gradients, such that [40]

$$H_o = \sqrt{3}\,\kappa\tau_S = \sqrt{3}\kappa\alpha_S G b_S \sqrt{\rho_S}. \tag{54}$$

With these relations we can now write the microhardness from the conical indenter using

Eqs. (50)–(54) as

$$\left(\frac{H}{H_o}\right)^{\beta} = 1 + \left(\frac{h^*}{h}\right)^{\beta/2}, \tag{55}$$

where h^* is a material specific parameter that characterizes the depth dependence of the hardness and depends on the indenter geometry as well as on the plastic flow, such that it is derived as

$$h^* = \zeta \ell \tag{56}$$

with

$$\zeta = \frac{3}{2c\bar{r}} \tan\theta. \tag{57}$$

Equation (56) shows that h^* is a linear function of the length-scale parameter ℓ. Thus, h^* is a crucial parameter, which characterizes the indentation size effects, and its accurate experimental measure gives a reasonable value for the length-scale parameter ℓ obtained by using Eq. (56). Moreover, substituting Eq. (53) into Eq. (54) along with Eq. (44), one can obtain a simple relation to predict the macrohardness H_o as

$$H_o = \kappa k \sqrt{c \tan\theta}, \tag{58}$$

where k can be obtained by using Eq. $(33)_3$. Equations (56) and (58) are similar to the phenomenological relations suggested by Yuan and Chen [44] based on finite element computations and the experimental results of Begley and Hutchinson [42]. Moreover, Eq. (58) can be used to determine the c parameter if H_o is provided from the indentation test. H_o corresponds to the saturation value where the hardness H does not change as the indentation depth h increases (or with further load increase) in the H versus h indentation test curve.

We note that if $\beta = 2$ in Eq. (55), one retains the relation originally proposed by Nix and Gao [40], where they found a linear dependence of the square of the microhardness H^2 to the inverse of the indentation depth $1/h$. Nix and Gao [40] also suggested that h^* and H_o are dependent and related through $h^* = (81/2)b\alpha^2 \tan^2\theta (G/H_o)^2$. Their relation thus gives a similar argument to that of Eq. (56), which suggests that h^* is dependent on the shape of the indenter as well as on the material property. Furthermore, Yuan and Chen [44] modified the Nix and Gao [40] relation by introducing another empirical term $(\varsigma^*/h)^2$ that is subtracted from the right-hand side of Eq. (55) with $\beta = 2$, where ς^* is another material parameter that depends on both material property and the indenter geometry. However, they showed numerically that the effect of this additional parameter ς^* is generally much smaller than h^*, and it can be neglected in many cases.

The characteristic form for the depth dependence of the hardness presented by Eq. (55) gives a straight line when the data are plotted as $(H/H_o)^{\beta}$ versus $h^{-\beta/2}$, the intercept of which is 1 and the slope is $h^{*\beta/2}$. Nix and Gao [40] showed for $\beta = 2$ that the plot of $(H/H_o)^2$ versus $1/h$ compares well with the experimental data from micro-indentation tests using a conical indenter. The length-scale parameter $\ell = h^*/\zeta$ can then be calculated using Eq. (56), where ζ is determined in terms of the shape of the conical indenter (i.e., $\tan\theta$) and the material properties (i.e., $\bar{r}$ and c), which are known. Therefore, by using Eq. (55) to fit the hardness experimental data obtained from indentation tests, one can simply compute the intrinsic length-scale parameter that characterizes the size effects using Eq. (56).

All the experiments used here in identifying the length-scale parameter ℓ were conducted at room temperature and using a Berkovich triangular pyramidal indenter for which the nominal or projected contact area varies as [78]

$$A_c = 24.5h^2 = \pi a^2. \tag{59}$$

Using this relation together with $\tan\theta = h/a$ yields

$$\tan\theta = \sqrt{\frac{\pi}{24.5}} = 0.358. \tag{60}$$

Note that it was reported by the experimentalists that no damage occurred in the material beneath the indenter such that the measured microhardness data provides a true measure of the plastic properties of the specimen. Microhardness thus provides a convenient tool for the identification of the plasticity intrinsic material length scale, where damage is avoided.

Following the method proposed by Nix and Gao [40], the hardness results obtained from microindentation tests can be displayed as a plot of $(H/H_o)^\beta$ versus $h^{-\beta/2}$, as shown for the (111) single-crystal copper and cold-worked polycrystalline copper in Fig. 2, for (100) and (110) single crystals of silver in Fig. 3, and annealed and work-hardened alpha brass in Fig. 4.

Table 1 shows the calculated values of ℓ for the six sets of indentation data described by Eq. (55) in Fig. 2–4. The ζ parameter is calculated by using Eq. (57), assuming that $c = 1.0$ [77] and the Nye factor $\bar{r} = 2$ [16]. The calculation of ℓ, however, depends strongly on the material parameters c and $\bar{r}$. The resulting values for the material intrinsic length scale outlined in Table 1 are in the range of some micrometers, which confirms well with the observations of Nix and Gao [40], Begley and Hutchinson [42], Stolken and Evans [9], and Yuan and Chen [44]. Moreover, one can note that ℓ for the cold-worked sample is smaller than the value for the annealed sample, indicating that spacing between statistically stored dislocations is reduced in the hardened-worked material. Similar result has been reported by Nix and Gao [40], and Stolkend and Evans [9]. Apparently, numerical experiments of the indentation problem using finite element method are required to verify those findings. However, this is not the subject of this study and will be shown in a forthcoming paper [33, 34].

It can be seen from the results that as the depth of indentation h becomes much larger than the material-length scale parameter ℓ, the gradient effects become smaller and the corresponding hardness does not exhibit any indentation size effect. Moreover, if the material is intrinsically hard (i.e., shallow indentation

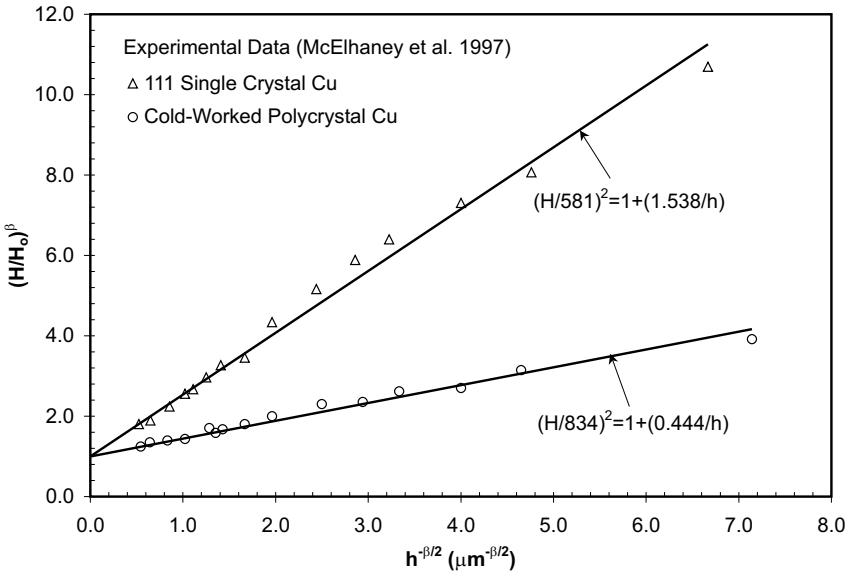

FIGURE 2. Comparison of the experimental results and the prediction of Eq. (55) to determine the intrinsic material length scale ℓ for copper

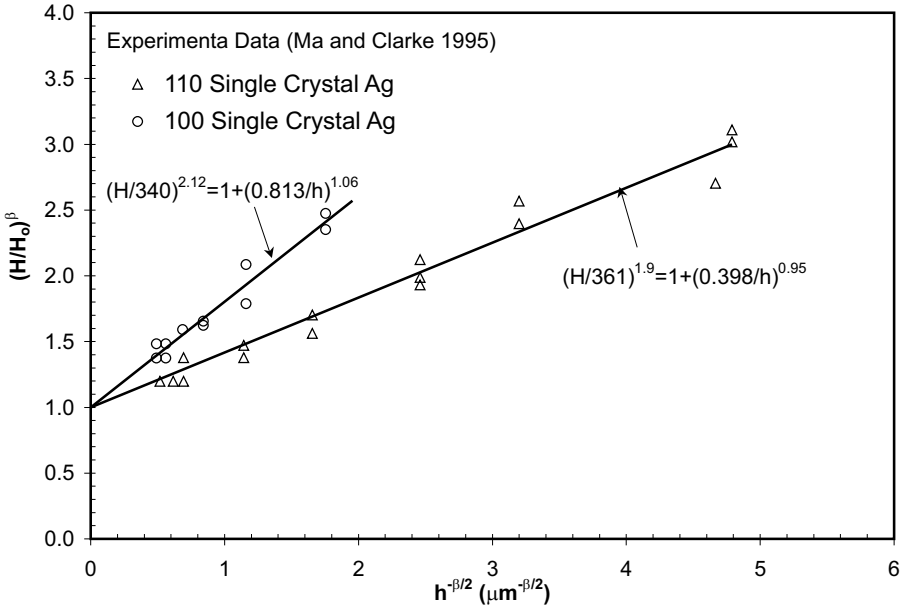

FIGURE 3. Comparison of the experimental results and the prediction of Eq. (55) to determine the intrinsic material length scale ℓ for silver

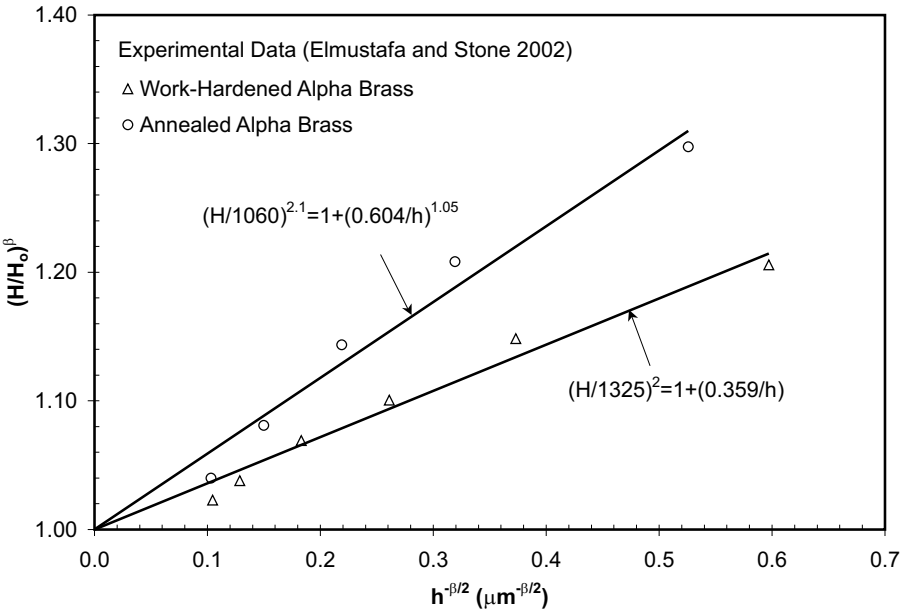

FIGURE 4. Comparison of the experimental results and the prediction of Eq. (55) to determine the intrinsic material length scale ℓ for alpha brass

Table 1. Calculation of the length-scale parameter ℓ from the fitted microhardness data

Material	β	H_o (MPa)	h^* (μm)	ζ (Eq. (57))	$\ell = h^*/\zeta$ (μm)
(111) single crystal Cu (annealed)	2.00	581	1.538	0.268	5.74 (12.00)[1] (20.00)[2]
Polycrystalline Cu (cold-worked)	2.00	834	0.444	0.268	1.66 (5.84)[1] (6.00)[2]
(100) signle crystal Ag	2.12	340	0.813	0.268	3.03 (0.34-0.39)[3]
(110) single crystal Ag	1.90	361	0.398	0.268	1.49 (0.19-0.22)[3]
Alpha brass (annealed)	2.10	1060	0.604	0.268	2.25
Alpha brass (cold-worked)	2.00	1325	0.359	0.268	1.34

[1] Nix and Gao [40]

[2] Yuan and Chen [44]

[3] Begley and Hutchinson [42]

depths or nanoindentation), the microhardness model given by Eq. (55) gives more accurate results than Nix and Gao [40] model. This improvement in the model predictions is attributed to β, which can be considered as a material parameter that depends on the crystal structure. The role of the material parameter β in the gradient plasticity models and in predicting the micro- and nanohardness have been studied thoroughly by Abu Al-Rub and Voyiadjis [45]. It is found that β constant, which assesses the coupling between statistically stored dislocations and geometrically necessary dislocations in Taylor's hardening law, plays a crucial role in correlating the hardness data from nano- and microindentations, where the Nix and Gao [40] model failed to do so. Apparently, further evelopments of the gradient plasticity theory are required.

Moreover, it is obvious that numerical experiments of the indentation problem are required to verify the above findings. Examples of two-dimensional verses three-dimensional indentation simulations can be found in a recent work by Muliana *et al*. [79]. In addition, numerical examples showing the effectiveness of the proposed equations in capturing the size-dependent behavior as compared to the experimental results are required. Examples for such problems are microbending of thin beams, microtorsion of thin wires, growth of microvoids, shear bands, and rate-dependent micro- and nanoindentation of thin films. However, this is not the subject of this study and will be addressed in a forthcoming work by the authors.

4. ON THE EVOLUTION OF THE MATERIAL-INTRINSIC LENGTH SCALE

The aforementioned conclusion in Section 2, which states that Eq. (34) or (44) implies that both the strain-rate effect and temperature variation are crucial to the reliability of the es-

timated length-scale parameter ℓ, motivates the following argument. To the authors' best knowledge, neither a numerical investigation nor an experimental study has been carried out for the influence of strain-rate effect and temperature variation on the strain-gradient plasticity, or more specifically, on the size effect exhibited by the presence of geometrically necessary dislocations. For example, the plastic zone ahead of the crack tip will decrease with increasing yield stress, which for small-scale yielding is of the order of microns. Therefore, the consideration of strain-rate effect and temperature variation on gradient plasticity, particularly in dynamic problems, becomes more necessary. Existing theories of gradient plasticity, however, have failed to explain such behavior. Equations (34) or (44) shows that ℓ is not constant for a given material, but is required to change as the flow stress in the absence of strain-gradient changes. This is crucial for the classical viscoplasticity theory since it cannot predict size effect, too. Therefore, the consideration of the evolution of the material intrinsic-length parameter with time ℓ in dynamic problems becomes more necessary. Moreover, there are indications that a constant value of the material length scale is not always realistic, and that different problems could require different values (see for example the work of Aifantis [80] and Tsagrakis and Aifantis [46]). Some authors argued the necessity of a length-scale parameter in the gradient theories that change with time in order to achieve an efficient computational convergence while conducting multiscale simulations [51].

The rate and temperature dependence of ℓ for metal crystals can be explained by different physical mechanisms of dislocation motion. Taking the time derivative of the general relation for ℓ, Eq. $(42)_4$, yields

$$\dot{\ell} = A v_S, \tag{61}$$

where $v_S = \dot{L}_S$ is the average dislocation speed and $A = (\alpha_G/\alpha_S)^2 (b_G/b_S)\, \bar{M}\, \bar{r}$. In obtaining Eq. (61), it was assumed that the slip system does not change with time such that the time derivative of the Burgers vector magnitude b, Schmidt's orientation factor $\bar{M}$, and the Nye factor $\bar{r}$ is zero. One might think that this assumption is limiting in that plastic strains, even in small deformation theory, will cause a material rotation and then strain-gradient evolution, as stated by Eq. (26), which is taken from the work of Fleck and Hutchinson [19]. Therefore, such an assumption implies that there is no change in the geometrically necessary dislocations; thus, the absence of strain-gradient changes. However, this assumption is imperative since we need to study the effect of strain rates and temperature variations on ℓ such that ℓ is not constant for a given material, but is required to change as the flow stress in the absence of strain gradient changes [see Eq. (25)].

Since plastic flow occurs by the motion of dislocations, the rate at which it takes place depends on how fast the dislocations move, how many dislocations are moving in a given volume, how much displacement is carried by each dislocation, and how much rotation each crystal undergoes. The theory of crystal dislocations shows that if a dislocation (in this case a statistically stored dislocation) is moving through rows of barriers formed by obstacle dislocations (in this case geometrically necessary dislocations), then its velocity can be determined from the following expression:

$$v_S = \frac{L_S}{t_w + t_t}, \tag{62}$$

where the total transient time of a dislocation is equal to the sum of the waiting time t_w spent at the obstacle and the travel time between obstacles t_t. If the ratio t_w/t_t increases, then the strain gradients become more important and the dislocation velocity v_S, in Eq. (62), can be approximated by the expression

$$v_S = \nu L_S, \tag{63}$$

where $\nu = 1/t_w$ is the frequency of successful jumps or the rate at which the SSDs overcome the GNDs. This is defined from statistical considerations as follows (e.g., [59, 81]):

$$\nu = \nu_o \exp\left(-\frac{U(\sigma^*)}{kT}\right), \tag{64}$$

where ν_o is the fundamental vibrational frequency of the dislocation (considerably lower than the vibrational frequency of the atom), k is the Boltzmann's constant, T is the absolute temperature, and U is the activation energy, which may depend not only on the applied thermal stress σ^* but also on the temperature and the internal structure. Expressions for the activation energy for various types of obstacles are given by Kocks *et al*. [56], where a generalized equation for these shapes with two parameters, a_1 and a_2, has been proposed,

$$U = U_o\left[1 - \left(\frac{\sigma^*}{\sigma_o^*}\right)^{a_1}\right]^{a_2}. \tag{65}$$

Substitution of Eqs. (63)–(65) into Eq. (61) along with Eq. $(42)_4$ gives the following expression for the evolution of the length-scale parameter $\dot{\ell}$ as

$$\dot{\ell} = \ell\nu_o \exp\left[-\frac{U_o}{kT}\left\{1 - \left(\frac{\sigma^*}{\sigma_o^*}\right)^{a_1}\right\}^{a_2}\right]. \tag{66}$$

This equation shows that ℓ is temperature dependent. Moreover, it is well known that the flow thermal stress σ^* of most metallic materials increases with strain rate, which also makes Eq. (66) strain-rate dependent. There are different empirical and physically based dynamic constitutive models that have been proposed to estimate the dynamic thermal flow stress σ^* for metallic materials at high-strain rates, which incorporate strain, strain rate, temperature, damage history, plastic strain rate history, dislocation dynamics, grain size, and other intrinsic variables (e.g., [81-84]). These models can be combined with Eq. (66) to study the size-effect phenomena in dynamic problems. Furthermore, when plasticity occurs (i.e., $\sigma^* = \sigma_o^*$, $\dot{\ell}$ becomes $\dot{\ell} = \ell\nu_o$, where ℓ is given as the estimate identified from microhardness results.

5. CONCLUSIONS

This paper addresses the problem of determining the intrinsic length-scale parameter of the gradient plasticity theory. The definition and magnitude of the intrinsic length scale are keys to the development of the new theory of plasticity that incorporates size effects. It also sets up the main assumptions to determine the length scales that will be essentially the basis for accurate qualitative and quantitative multiscale modeling, simulation, and design of emerging micro- and nanosystems. Two different micromechanical flow stress models to assess the coupling between statistically stored dislocations (SSDs) and geometrically necessary dislocations (GNDs) are discussed. One in which the SSDs and GNDs are simply summed (model-I) and one in which, implicitly, their accompanying strengths are added (model-II). These two dislocation interaction models, which are based on Taylor's hardening law, are used to identify the deformation-gradient-related intrinsic length-scale parameter ℓ in terms of measurable microstructural physical parameters. This is done through using the gradient theory to bring the microstructural (described by Taylor's hardening law) and continuum (described by the strain-hardening power law) descriptions of plasticity closer together. As a result ℓ is defined in terms of the average distance between statistically stored dislocations L_S (characterizes the characteristic length of plasticity phenomenon), the Nye factor $\bar{r}$ (characterizes the microstructure dimension, e.g., grain size, grain boundary width, obstacle spacing, and radius), Schmidt's orientation factor $\bar{M}$ (characterizes the lattice rotation), the Burgers vector b

(characterizes the displacement carried out by each dislocation), and the empirical constant α (characterizes the deviation from regular spatial arrangement of the SSD or GND populations).

While such an increasing interest in gradient-enhanced theories can be understood in view of the aforementioned remedies they provided, actual experiments for the direct measurement of the material-intrinsic length parameter introduced by the phenomenological gradient coefficients are lacking. When considering the microstructure with localization zones, gradient-dependent behavior is expected to become important once the length scale associated with the local deformation gradients becomes sufficiently large when compared with the characteristic dimension of the system. It follows that such experiments could be difficult to design and interpret. However, microhardness tests provide a method to determine the material-intrinsic length-scale parameter ℓ in the gradient plasticity models.

This paper, therefore, provides an initial effort in this direction, where we discuss the issue of size effect and the calibration of gradient theory in terms of micro- and nanoindentation experiments to determine the value of the material-intrinsic length parameter that scales the gradient effects. We show, in particular, that gradient plasticity models can be used for the interpretation of size effect experiments in micro- and nanoindentation. In fact, the aforementioned gradient models are calibrated by fitting the corresponding length-scale parameter to the experimental data. Micro- and nanoindentation tests can thus be used for the experimental determination of the gradient length-scale parameter. Moreover, an evolution law has been derived for the intrinsic-material length scale ℓ in gradient plasticity in terms of the flow stress and temperature. This law suggests that the material-intrinsic length scale decreases with increasing strain rates, and increases with temperature. However, additional experimental measurements and numerical investigations are needed to fully verify the derived micromechanical equations for the material intrinsic length parameter ℓ.

The gradient law proposed in Eq. (25) is based on dislocation-mechanics considerations, which is a departure from all the current gradient theories that are based on the ideal assumption of all the obstacles being equally strong and equally spaced along a straight or curved contacting line (i.e., $\rho_T = \rho_S + \rho_G$). The real situation in experiments suggests that the hardening law cannot be taken as a simple sum of the densities of SSDs and GNDs such that $\rho_T = \left[\rho_S^\beta + \rho_G^\beta\right]^{1/\beta}$.This general form of the gradient plasticity theory encompasses most of the gradient plasticity theories found in the open literature and forms a promising basis for future multiscale computations. In addition, this model gives an alternative framework that could model size-dependent plasticity without higher-order stresses or additional boundary conditions, so as to preserve the essential structure of classical plasticity. This approach has the advantages that it is simpler overall and can be easily implemented into existing finite element codes.

Finally, no one up until now can claim that he obtained the actual material-intrinsic length scale because of the lack of experimental procedures to do so and the lack of solid physical interpretations of the material-intrinsic length scale. Therefore, there still an open question for researchers: What is the physical interpretation of the constitutive length parameter ℓ?

ACKNOWLEDGMENT

The authors gratefully acknowledge the financial support by the Air Force Institute of Technology, at Wright Patterson Air Force Base, Ohio.

REFERENCES

1. Lloyd, D.J. Particle reinforced aluminum and magnesium matrix composites. *Int. Mater. Rev.* **39**:1–23, 1994.
2. Rhee, M., Hirth, J.P., and Zbib, H.M. A superdislocation model for the strengthening of metal matrix composites and the initiation and propagation of shear bands. *Acta Metall. Mater.* **42**:2645–2655, 1994.
3. Rhee, M., Hirth, J.P., and Zbib, H.M. On the bowed out tilt wall model of flow stress and size effects in metal matrix composites. *Scripta Metall. Mater.* **31**:1321–1324, 1994.
4. Zhu, H.T., and Zbib, H.M. Flow strength and size effect of an Al–Si–Mg composite model system under multiaxial loading. *Scripta Metall. Mater.* **32**:1895–1902, 1995.
5. Nan, C.-W., and Clarke, D.R. The influence of particle size and particle fracture on the elastic/plastic deformation of metal matrix composites. *Acta Mater.* **44**:3801–3811, 1996.
6. Kiser, M.T., Zok, F.W., and Wilkinson, D.S. Plastic flow and fracture of a particulate metal matrix composite. *Acta Mater.* **44**:3465–3476, 1996.
7. Zhu, H.T., Zbib, H.M., and Aifantis, E.C. Strain gradients and continuum modeling of size effect in metal matrix composites. *Acta Mechan.* **121**:165–176, 1997.
8. Fleck, N.A., Muller, G.M., Ashby, M.F., and Hutchinson, J.W. Strain gradient plasticity: theory and experiment. *Acta. Metallurgica et Materialia* **42**:475–487, 1994.
9. Stolken, J.S., and Evans, A.G. A microbend test method for measuring the plasticity length-scale. *Acta Mater.* **46**:5109–5115, 1998.
10. Stelmashenko, N.A., Walls, M.G., Brown, L.M., and Milman, Y.V. Microindentation on W and Mo oriented single crystals: an STM study. *Acta Metall. Mater.* **41**:2855–2865, 1993.
11. De Guzman, M.S., Neubauer, G., Flinn, P., and Nix, W.D. The role of indentation depth on the measured hardness of materials. *Mater. Res. Symp. Proc.* **308**:613–618, 1993.
12. Ma, Q., and Clarke, D.R. Size dependent hardness in silver single crystals. *J. Mater. Res.* **10**:853–863, 1995.
13. McElhaney, K.W., Valssak, J.J., and Nix, W.D. Determination of indenter tip geometry and indentation contact area for depth sensing indentation experiments. *J. Mater. Res.* **13**:1300–1306, 1998.
14. Elmustafa, A.A., and Stone, D.S. Indentation size effect in polycrystalline F.C.C metals. *Acta Mater.* **50**:3641–3650, 2002.
15. Hill, R. *Mathematical Theory of Plasticity*, Oxford University Press, Oxford, 1950.
16. Arsenlis, A., and Parks, D.M. Crystallographic aspects of geometrically-necessary and statistically-stored dislocation density. *Acta Mater.* **47**:1597–1611, 1999.
17. Gao, H., Huang, Y., and Nix, W.D. Modeling plasticity at the micrometer scale. *Naturwissenschaften* **86**:507–515, 1999.
18. Ashby, M.F. The deformation of plastically non-homogenous alloys. *Phil. Mag.* **21**:399–424, 1970.
19. Fleck, N.A., and Hutchinson, J.W. Strain gradient plasticity. *Adv. Appl. Mech.* **33**:295–361, 1997.
20. Voyiadjis, G. Z., Aifantis, E. C., and Weber, G. Constitutive modeling of plasticity in nanostructured materials. In *Nano-Scale Mechanics of Nanostructured Materials for the LaRC Nanotechnology Program - NASA*, Kluwer Academic Publishers, Dordrecht, 2003.
21. Aifantis, E.C. On the microstructural origin of certain inelastic models. *J. Eng. Mater. Technol.* **106**:326–330, 1984.
22. Lasry, D., and Belytschko, T. Localization limiters in transient problems. *Int. J. Solids Struct.* **24**:581–597, 1988.
23. Mühlhaus, H.B., and Aifantis, E.C. A variational principle for gradient plasticity. *Int. J. Solids Struct.* **28**:845–857, 1991.
24. Kroner, E. Elasticity theory of materials with long range cohesive forces. *Int. J. Solids Struct.* **24**:581–597, 1967.
25. Eringen, A.C., and Edelen, D.G.B. On non-local elasticity. *Int. J. Eng. Sci.* **10**:233–248, 1972.
26. Pijaudier-Cabot, T.G.P., and Bazant, Z.P. Nonlocal damage theory. *ASCE J. of Engng. Mech.* **113**:1512–1533, 1987.
27. de Borst, R., and Mühlhaus, H.-B. Gradient-

dependent plasticity formulation and algorithmic aspects. *Int. J. Numer. Met. Engng.* **35**:521–539, 1992.

28. Fleck, N.A. and Hutchinson, J.W. A reformulation of strain gradient plasticity. *J. Mech. Phys. Solids* **49**:2245–2271, 2001.
29. Peerlings, R.H.J., de Borst, R., Brekelmans, W.A.M., and de Vree, J.H.P. Gradient enhanced damage for quasi-brittle materials. *Int. J. Numer. Met. Engng.* **39**:3391–3403, 1996.
30. Kuhl, E., Ramm, E., and de Borst, R. An anisotropic gradient damage model for quasi-brittle materials. *Comp. Met. Appl. Mech. Eng.* **183**:87–103, 2000.
31. Voyiadjis, G.Z., Deliktas, B., and Aifantis, E.C. Multiscale analysis of multiple damage mechanics coupled with inelastic behavior of composite materials. *ASCE J. Eng. Mech.* **127**(7):636–645, 2001.
32. Voyiadjis, G.Z., and Dorgan, R.J. Gradient formulation in coupled damage-plasticity. *Arch. Mech.* **53**(4-5):565–597, 2001.
33. Voyiadjis, G.Z., Abu Al-Rub, R.K., and Palazotto, A.N. Non-local coupling of viscoplasticity and anisotropic viscodamage for impact problems using the gradient theory. *Arch. Mech.* **55**(1):39–89, 2003.
34. Voyiadjis, G.Z., Abu Al-Rub, R.K., and Palazotto, A.N. Thermodynamic formulations for non-local coupling of viscoplasticity and anisotropic viscodamage for dynamic localization problems using gradient theory. *Int. J. Plasticity* (in press).
35. Shu, J.Y., and Fleck, N.A. Strain gradient crystal plasticity: Size dependent deformation in bicrystals. *J. Mech. Phys. Solids* **47**:297–324, 1999.
36. Shu, J.Y., and Barrlow, C.Y. Strain gradient effects on microscopic strain field in a metal matrix composite. *Int. J. Plasticity* **16**:563–591, 2000.
37. Busso, E.P., Meissonnier, F.T., and O'Dowd, N.P. Gradient-dependent deformation of two-phase single crystals. *J. Mech. Phys. Solids* **48**:2333–2361, 2000.
38. Bassani, J.L. Incompatibility and a simple gradient theory of plasticity. *J. Mech. Phys. Solids* **49**:1983–1996, 2001.
39. Xue, Z., Huang, Y., and Li, M. Particle size effect in metallic materials: a study by the theory of mechanism-based strain gradient plasticity. *Acta Mater.* **50**:149–160, 2002.
40. Nix, W.D., and Gao, H. Indentation size effects in crystalline materials: a law for strain gradient plasticity. *J. Mech. Phys. Solids* **46**(3):411–425, 1998.
41. Shu, J.Y., and Fleck, N.A. The prediction of a size effect in micro-indentation. *Int. J. Solids Struct.* **35**:1363–1383, 1998.
42. Begley, M.R., and Hutchinson, J.W. The mechanics of size-dependent indentation. *J. Mech. Phys. Solids* **46**:2049–2068, 1998.
43. Huang, Y., Xue, Z., Gao, H., and Xia, Z.C. A study of micro-indentation hardness tests by mechanism-based strain gradient plasticity. *J. Mat. Res.* **15**:1786–1796, 2000.
44. Yuan, H., and Chen, J. Identification of the intrinsic material length in gradient plasticity theory from micro-indentation tests. *Int. J. Solids Struct.* **38**:8171–8187, 2001.
45. Abu Al-Rub, R.K., and Voyiadjis, G.Z. Analytical and experimental determination of the material intrinsic length scale of strain gradient plasticity theory from micro- and nano-indentation experiments. *Int. J. Plasticity* (in press).
46. Tsagrakis, I., and Aifantis, E.C. Recent developments in gradient plasticity-Part I: formulation and size effects. *ASME Trans., J. Eng. Mat. Tech.* **124**:352–357, 2002.
47. de Borst, R., Sluys, L.J., Mühlhaus, H.-B., and Pamin, J. Fundamental issues in finite element analysis of localization of deformation. *Eng. Comp.* **10**:99–121, 1993.
48. Bammann, D.J., Mosher, D., Hughes, D.A., Moody, N.R., and Dawson, P.R. *Using Spatial Gradients to Model Localization Phenomena*, Sandia National Laboratories Report, SAND99-8588, Albuquerque, NM, and Livermore, CA, 1999.
49. Poole, W.J., Ashby, M.F., and Fleck, N.A. Microhardness of annealed and work-hardened copper polycrystals. *Scripta Mater.* **34**(4):559–564, 1996.
50. Voyiadjis, G. Z., and Abu Al-Rub R. K. Length scales in gradient plasticity. In *Multiscale Model-*

ing and Characterization of Elastic-Inelastic Behavior of Engineering Materials, Morocco, October, Ahzi, S., and Cherkaoui, M., Eds. Kluwer Academic Publishers, Dordrecht, 8 pages, 2002.

51. Pamin, J. Gradient-Dependent Plasticity in Numerical Simulation of Localization Phenomena, Ph.D. dissertation, Delft University Press, The Netherlands, 1994.
52. Aifantis, E.C. The physics of plastic deformation. *Int. J. Plasticity* **3**:211–247, 1987.
53. Huang, Y., Gao, H., Nix, W.D., and Hutchinson, J.W. Mechanism-based strain gradient plasticity - II Analysis. *J. Mech. Phys. Solids* **48**:99–128, 2000a.
54. Gao, H., Huang, Y., Nix, W.D., and Hutchinson, J.W. Mechanism-based strain gradient plasticity - I. Theory. *J. Mech. Phys. Solids* **47**(6):1239–1263, 1999a.
55. Smyshlyaev, V.P., and Fleck, N.A. The role of strain gradients in the grain size effect for polycrystals. *J. Mech. Phys. Solids* **44**:465–495, 1996.
56. Kocks, U.F., Argon, A.S., and Ashby, M.F. *Thermodynamics and Kinetics of Slip*, Oxford, 1975.
57. Kroner, E. Dislocations and continuum mechanics. *Appl. Mech. Rev.* **15**:599–606, 1962.
58. Kucharski, S., and Mroz, Z. Identification of plastic hardening parameters of metals from spherical indentation tests. *Mater. Sci. Eng.* **A318**:65–76, 2001.
59. Bammann, D.J., and Aifantis, E.C. On a proposal for a continuum with microstructure. *Acta Mech.* **45**:91–121, 1982.
60. Bammann, D.J., and Aifantis, E.C. A model for finite-deformation plasticity. *Acta Mech.* **69**:97–117, 1987.
61. Columbus, D., and Grujicic, M. A A comparative discrete-dislocation/nonlocal crystal-plasticity analysis of plane-strain mode I fracture. *Mater. Sci. Eng.* **A323**:386–402, 2002.
62. Kocks, U.F. A statistical theory of flow stress and work hardening. *Phil. Mag.* **13**:541, 1966.
63. Tabor, D. *The Hardness of Metals*, Clarendon Press, Oxford, 1951.
64. Atkins, A.G., and Tabor, D.T. Plastic indentation in metals with cones. *J. Mech. Phys. Solids* **13**:149–164, 1965.
65. Biwa, S., and Storakers, B. An analysis of fully plastic Brinell indentation. *J. Mech. Phys. Solids* **43**(8):1303–1333, 1995
66. Robinson, W.H., and Truman, S.D. Stress-strain curve for aluminum from a continuous indentation test. *J. Mater. Sci.* **12**(1):1961–1965, 1977.
67. Tangena, A.G., and Hurkx, G.A.M. Determination of stress-strain curves of thin layers using indentation tests. *ASME J. Eng. Mater. Technol.* **108**(3):230–232, 1986.
68. Huber, N., and Tsakmakis, Ch. Determination of constitutive properties from spherical indentation data using neural networks. Part II: plasticity with nonlinear isotropic and kinematic hardening. *J. Mech. Phys. Solids* **47**:1589–1607, 1999.
69. Caceres, C.H., and Poole, W.J. Hardness and flow strength in particulate metal matrix composites. *Mater. Sci. Eng.* **A332**:311–317, 2002.
70. Swadener, J.G., George, E.P., and Pharr, G.M. The correlation of the indentation size effect measured with indenters of various shapes. *J. Mech. Phys. Solids* **50**:681–694, 2002.
71. Oliver, W.C., Pharr, G.M. An improved technique for determining hardness and elastic modulus using load and displacement sensing indentation experiments. *J. Mater. Res.* **7**:1564–1583, 1992.
72. Hill, R., Storakers, B., and Zdunek, A.B. A theoretical study of the Brinell hardness test. *Proc. Roy. Soc. (London)* **A423**(1865):301–330, 1989.
73. Xue, Z., Huang, Y., Hwang, K.C., and Li, M. The influence of indenter tip radius on the micro-indentation hardness. *ASME J. Eng. Mater. Technol.* **124**:371–379, 2002.
74. McClintock, F.A., and Argon, A.S. *Mechanical Behavior of Materials*, Addison-Wesley Publishing Company, Reading, MA, 1966
75. Muliana, A., Steward, R., Haj-Ali, R., Saxena, A. Artificial neural network and finite element modeling of nanoindentation tests. *Metallurgical and Materials Transactions* **A33**:1939–1947, 2002.
76. Aifantis, E.C. Strain gradient interpretation of size effects. *Int. J. Fract.* **95**:299–314, 1999.
77. Mayers, M.A., Benson, D.J., Vohringer, O., Kad, B.K., Xue, Q., and Fu, H.-H. Constitutive de-

scription of dynamic deformation: physically-based mechanisms. *Mater. Sci. Eng.* **A322**:194–216, 2002.

78. Johnson, G.R., and Cook H. W. Fracture characteristics of three metals subjected to various strains, strain rates, temperature and pressures. *Engng. Fract. Mech.* **21**(1):31–48, 1985.
79. Zerilli, F.J., and Armstrong, R.W. Dislocation-mechanics-based constitutive relations for material dynamics calculations. *J. App. Phys.* **61**(5):445–459, 1987.
80. Steinberg, D.J., and Lund, C.M. A constitutive model for strain rates from 10^{-4} to 10^{6}. *J. App. Phys.* **65**(4):1528–1533, 1989.